Journal of Alloys and Compounds 509 (2011) 9663–9668

Contents lists available at ScienceDirect

Journal of Alloys and Compounds

journal homepage: www.elsevier.com/locate/jallcom

Kinetics of picosecond laser treatment of silver nanoparticles on ITO substrate

K. Nouneh[a,b], M. Oyama[b], G. Lakshminarayana[c,*], I.V. Kityk[d], A. Wojciechowski[d], K. Ozga[e]

[a] INANOTECH, Institute of Nanomaterials and Nanotechnology, MAScIR (Moroccan Advanced Science, Innovation and Research Foundation), ENSET, Av. Armée Royale, 10100 Rabat, Morocco
[b] Graduate School of Engineering, Kyoto University, Nishikyo-ku, Kyoto 615-8520, Japan
[c] Materials Science and Technology Division (MST-7), Los Alamos National Laboratory, Los Alamos, NM 87545, USA
[d] Electrical Engineering Department, Czestochowa University of Technology, Al. Armii Krajowej 17/19, 42-200 Czestochowa, Poland
[e] Chair of Public Health, Czestochowa University of Technology, Al. Armii Krajowej 36B, 42-200 Czestochowa, Poland

ARTICLE INFO

Article history:
Received 28 May 2011
Accepted 21 July 2011
Available online 28 July 2011

Keywords:
Nanoparticles
Surface plasmon resonance
Photoinduced absorption

ABSTRACT

In this work, the effect of ITO substrate on Ag NP size, morphology and photoinduced absorption depending on the time of 30 ps laser treatment were explicitly studied. Silver nanoparticles with an average diameter of ~40 nm supported on indium tin oxide (ITO) were irradiated with a tightly focused pulsed laser (doubled frequency beam) at 532 nm. The size transformation of silver nanoparticles induced by a single pulse of Nd:YAG laser (λ = 532 nm, pulse width = 30 ps) was directly observed by an electron scanning microscopy (FE-SEM) on indium tin oxide surface. Simultaneously the change in the absorption and the corresponding derivatives are also presented. These morphological changes are accompanied by a significant change in the optical absorption properties of the array. This study demonstrates that picosecond laser irradiation is an excellent technique to operate and control the properties of nanostructured materials on solid supports.

1. Introduction

Deposition of Ag nanoparticles onto indium tin oxide films (Ag-ITO) could vary the conductivity of transparent oxide which is very crucial for the optoelectronic applications [1]. The incorporation of silver nanoparticles could decrease the crystallization temperature and inhibits the growth of indium oxide. Recently, we have investigated the formation of uniform silver nanoparticles (AgNPs) on indium tin oxide (ITO) thin films deposited on glass substrate [2]. We have observed that the surface energy and the contact angle during the seed and growth process is one of the crucial factors that influence the size of the nanoparticles and their final physical properties. It showed clearly that the smooth region decreases the contact angle. As the NPs grow, the aggregation can easily occur due to the Ostwald ripening phenomenon by which the larger AgNPs grow at the expense of the smaller ones. The observed differences are attributed to the cavities existing between large grains and subgrains of ITO substrate. Further, Guillén et al. [3] have also described that the transmittance and sheet resistance values are prevailingly sensitive to the Ag film thickness; whereas the spectral range at which the maximum transmittance is carried out by appropriate adjusting of the ITO film thickness. Such features allow operating of their electronic properties through external laser induced treatment [4]. In Ref. [5] an efficient photo-induced phenomena to manipulate the average sizes and heights of silver nanoparticles deposited on transparent and conductive substrates through seed-mediated growth method are proposed. The substrate resistance was the main reason for the observed photo-induced aggregation features. The pico-second kinetics of photo-transparency engenders temporary oscillations and plays a principal role because of their commensurable with electron–phonon interactions, that determines the occurrence of the periodical structure of the silver nanoparticle sizes [5,6].

In this paper we present the principal results of the photo-induced absorption and modification of the surfaces of such films during the long-term sample's treatment with lasers.

2. Experimental

The attachment of AgNPs on ITO substrate was achieved by the seed-mediated growth method, allowing the fabrication of homogeneous dense and uniform AgNPs on ITO [2,7]. In the present work, at the beginning an ITO substrate was immersed during 2 h in a seed solution possessing 4 nm sizes of Ag nanoparticles, which were fabricated by the $NaBH_4$ reduction of $AgNO_3$ with trisodium citrate. After, the ITO surfaces were washed with pure water and dried in nitrogen atmosphere. The ITO was immersed for 2 h in a growth solution, containing $AgNO_3$, ascorbic acid, NaOH and cetyltrimethylamonium bromide, respectively. Through this two-step process, AgNP were attached on ITO and glass substrate [2,7]. Two types of ITO substrates were used in this work. ITO-4 Ω, and ITO-50 Ω substrates were produced by Kuramoto Seisakusho Co., Ltd. Japan, whose resistivity was ca. 4 Ω/square and 50 Ω/square, respectively, sputtered on glass substrate.

The JEOL JSM-7400F field emission scanning electron microscopy (FE-SEM) instrument, SEIKO SPA-400 atomic force microscopy (AFM) in tapping mode,

* Corresponding author. Tel.: +1 5056651804; fax: +1 5056655849.
E-mail address: glnphysics@rediffmail.com (G. Lakshminarayana).

0925-8388/$ – see front matter © 2011 Elsevier B.V. All rights reserved.
doi:10.1016/j.jallcom.2011.07.073

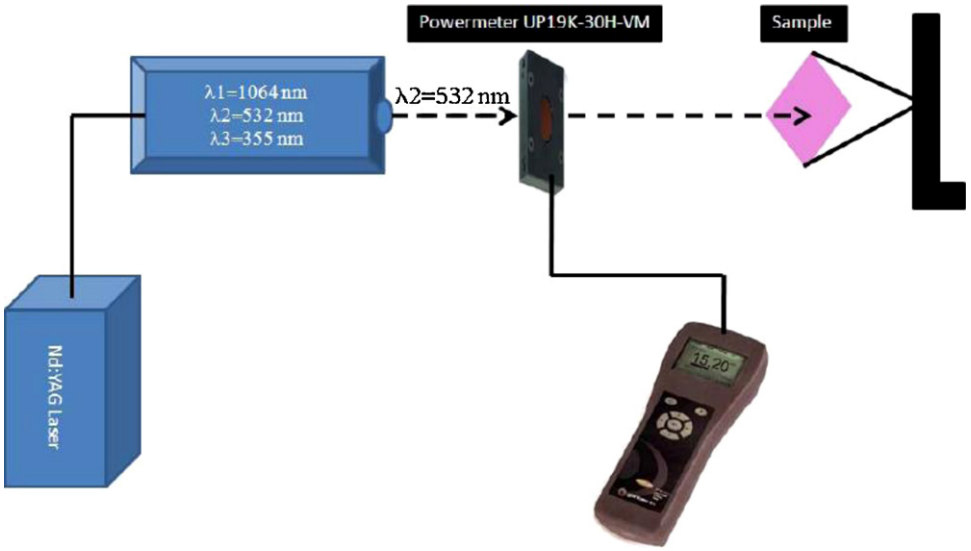

Fig. 1. Experimental setup of the Nd:YAG laser treatment used in this study.

Zeta-Sizer nano (Malvern instrument Ltd.) and UV/Vis/NIR (PerkinElmer Instrument Ltd.) spectroscopy were applied to monitor the growth of the silver nanoparticles in aqueous solution and on the ITO surface.

Photoinduced pulsed laser beams possessing 30 ps in duration were generated by compact Nd:YAG lasers (Continuum, Minilite), at the doubled frequency mode (532 nm) with a repetition rate of 10 Hz. The pulse energy was measured using Gentec-EO SOLO Power-meter UP19K-30H-VM in real time and adjusted to achieve lower energy (~20 mJ). The power densities used are calculated using the equation: $W = E/S$ (mJ/cm^2) where $S = \pi d^2/4$, and $d = 3$ mm is the diameter of output beam (see Fig. 1).

3. Results and discussion

Fig. 2 shows typical FE-SEM micrographs for the samples possessing 4 Ω/sq sheet, and 50 Ω/sq resistivity. By appropriate changes to the seed-mediated growth method, the surface of the ITO was modified. Their EDAX spectra are given in Fig. 3. Here the AgNPs are attached to the ITO substrates without using peculiar bridging reagents. The particle diameter, zeta-potential and electrophoretic mobility of the silver nanoparticle was measured by using an electrophoretic light scattering spectrometer equipped with a dynamic light scattering cell. The particle size distribution based on the light scattering intensity is plotted in Fig. 4. The average diameter of silver nanoparticles dispersed in aqueous solution was determined to be about 10 nm. The silver colloidal solution was very stable as indicated by zeta-potential distribution ($\zeta = -48.7$ mV) with a good electrophoretic mobility (-3.816 μm cm/Vs).

Following Fig. 5 one can clearly observe the changes of the shape of the particular Ag NP. Generally such changes are caused by photopolarization near the surface plasmon resonance (SPR) and by photothermal treatment which changes interaction between the particular Ag NP and ITO substrate. In fact, the excitation of large number of free carriers near the SPR spectral maximum will change the electrostatic inter-particle interactions that can affect the Ag NP leading to the reaction with oxygen, also due to high conductivity of the ITO substrate. However, the study of absorption in the vicinity of 520 nm, SPR maxima does not show significant changes. Thus in this case the specific morphology may form different effective surfaces of the nanograins which in turn may lead to different numbers of surface grain originated levels that are trapped into the energy range of the ITO substrate energy gap. As a consequence the photoinduced excitation near the SPR should lead to effective interactions between the large number of free carriers formed by plasmons and the trapping levels. Due to the long-time relaxation processes of corresponding metastable states, these processes are observed even after switching off the external light.

Fig. 6 presents the absorption spectra of silver nanoparticles coated on the Ag/ITO film. The measurements are presented for three different times of treatment by the same laser. From this figure it is clearly observed that there are some aggregates, which may have a substantial role on the transport of the carriers between the metallic NP and the ITO substrate. During the photo-excitation of the 532 nm (30 ps) laser beam, electrons and holes correspondingly are formed which are transferred to the borders with dielectric ITO. Increasing aggregation leads to the continuation of the process of the carrier trapping even after the switching off the induced laser.

Following Fig. 7, one can see that the increase in photo-induced time leads to a decrease of photo-absorption at 350 nm corresponding to the near band gap states of ITO. Moreover, with an increasing time of the cw laser treatment the induced absorption minimum also increased. The principal changes are observed on the border's regions separating Ag NP and ITO substrate and two spectral minima at 349 nm and 430 nm are observed. Interface states on the ITO energy gap and the Ag NP form the large number of trapping states under the illumination by 532 green light that show substantial photopolarization. More interestingly, even after the switching off the photo-induced treatment the process is continued. This phenomenon can be used for the dynamical operation of the absorption in this type of substrate. The separately performed photo-induced changes for the low resistance sheets 4 Ω/square are substantially less (not shown here), which confirm a principal role of the dielectric barriers for the accumulation of the charges. Maximal photo-induced absorption was observed for the 532 nm laser treatment time equal to about 15 min, and also switching off the illumination after 38 min. After this time duration we have observed a relatively slow decrement in the occurred photo-induced maxima. The observed maxima are caused by photo-induced polarization of the trapping levels and their effective interactions with the surface plasmon resonances typically for the seeded Ag NP at about 4 nm. Additional changes of the surface topology by laser treatment favors the formation of these trapping levels (see Fig. 5). Also the maximum decrease in the absorption spectra was achieved for picosecond's time of treatment equal to about 15 min. These maxima of the photo-induced absorption

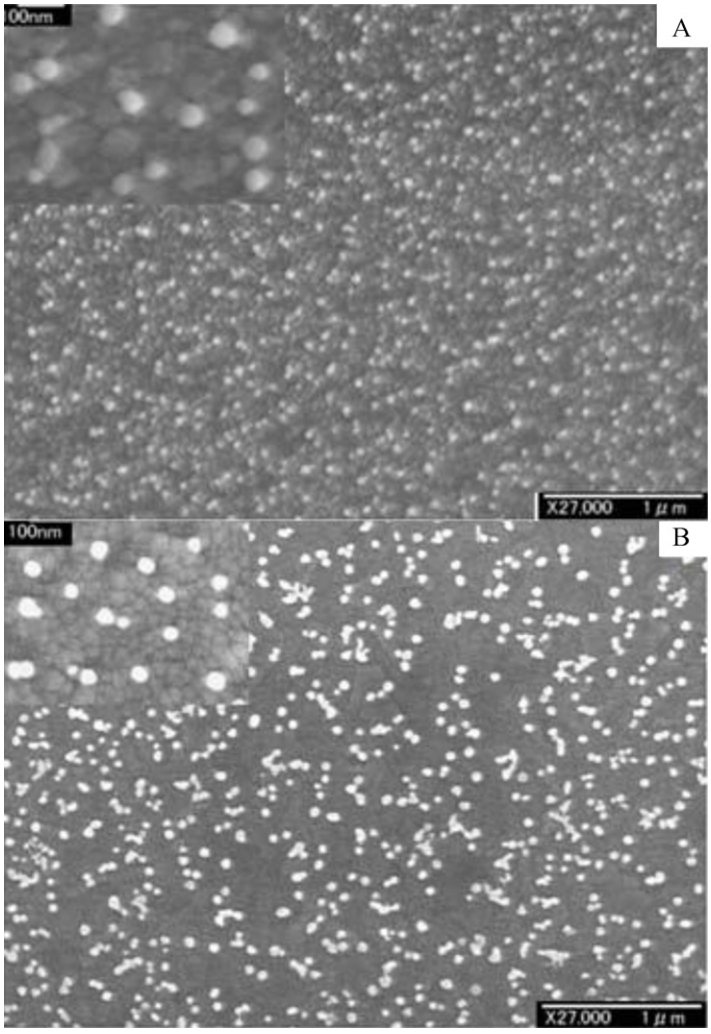

Fig. 2. FE-SEM images of the attached AgNPs on ITO substrates used in this study: A (50 Ω/sq) and B (4 Ω/sq).

are observed at wavelengths equal to about 340 and 355 nm, and switching off the laser treatment did not interrupt the process initiated even after 40 min. The photoinduced effects are observed near the cut-off absorption edge of ITO and on the short wavelength edge of the SPR. Such coexistence is caused by overlap of energies corresponding to large number of trapping levels on the border ITO-Ag NP and the broadened SPR due to the size dispersion. The clear enhancement of the photoinduced changes was observed only after the 3–5 min laser treatment. This is a consequence of the different localization of the photo-induced carriers on the borders separating the ITO substrate and the Ag NP SPR excitations due to the size dispersion.

Fig. 8 shows the AFM images of ITO-50 Ω/sq with different irradiation times. The morphological changes monitored by AFM show drastically increment of the Ag NP aggregations, which are responsible for the kinetics of the photo-induced treatments for such types of samples. The sheet resistivity of the ITO plays a principal role both for the morphology of the silver nanoparticles as well as for the polarizability of the main trapping levels determined by the resistance of the ITO substrate. This could be used for the operation through their photo-transparency features. More interestingly a continuation of the process even after the switching off the treatment was noticed (see the dependence after 15 min).

To understand the observed photoinduced dependence, it is necessary to take into account that during the seed process the solution undergoes de-wetting and then crystallization, but the generated small domains suffer from small inter-domain distance and interact *via* Van Der Waals forces and Oswald ripening that favor coalescence. In fact, the molecules at the surface of small particles are energetically not favored with respect to the molecules inside the bulk. To overcome this frustrated and unstable thermodynamic state, the surface molecules will detach from the surface and diffuse to join the neighboring particles, which leads to the

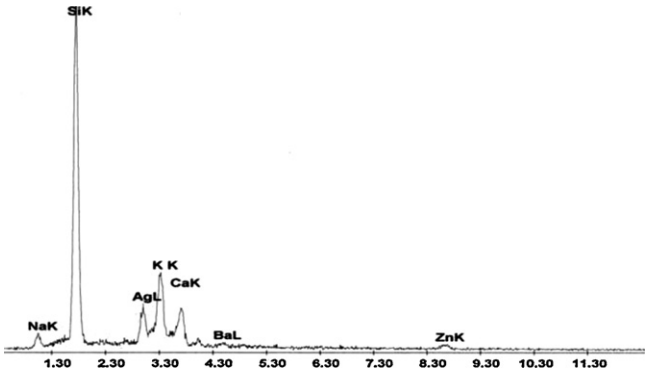

Fig. 3. EDAX measurements of Ag/ITO for the sample A (50 Ω/sq).

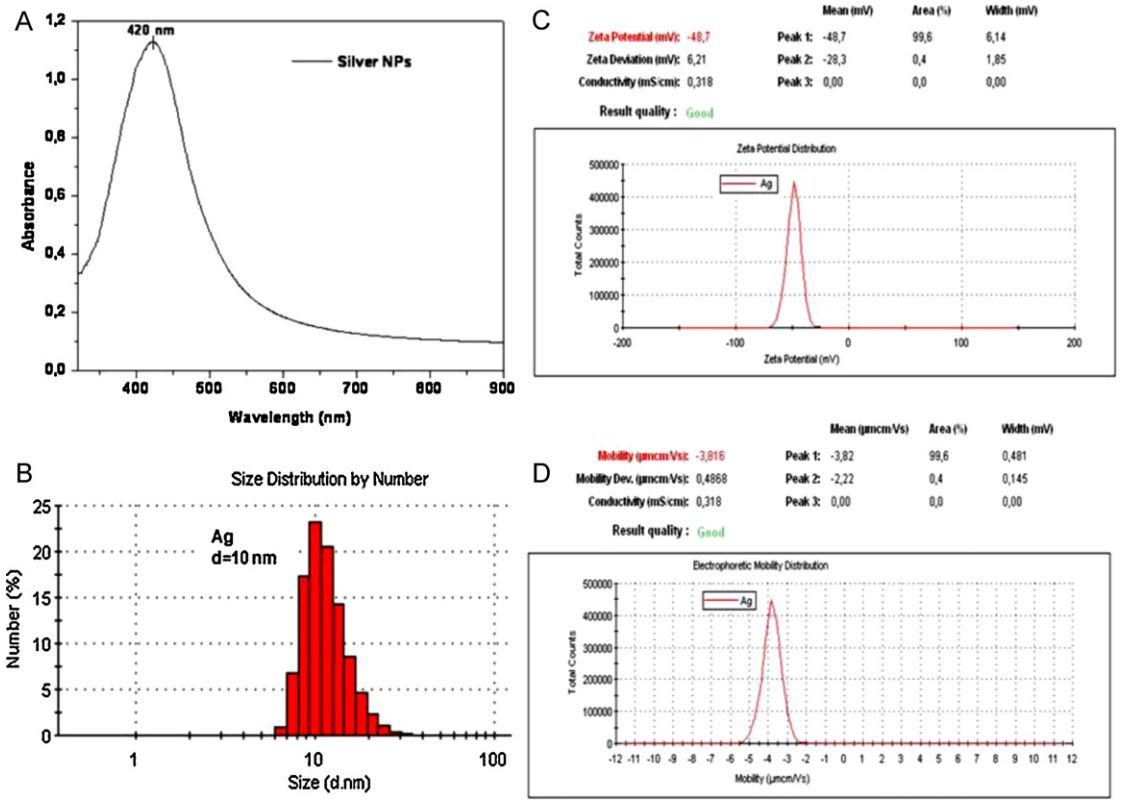

Fig. 4. Characterization of the silver nanoparticles: (A) absorbance spectrum; (B) size distribution; (C) zeta potential and (D) electrophoretic mobility distribution.

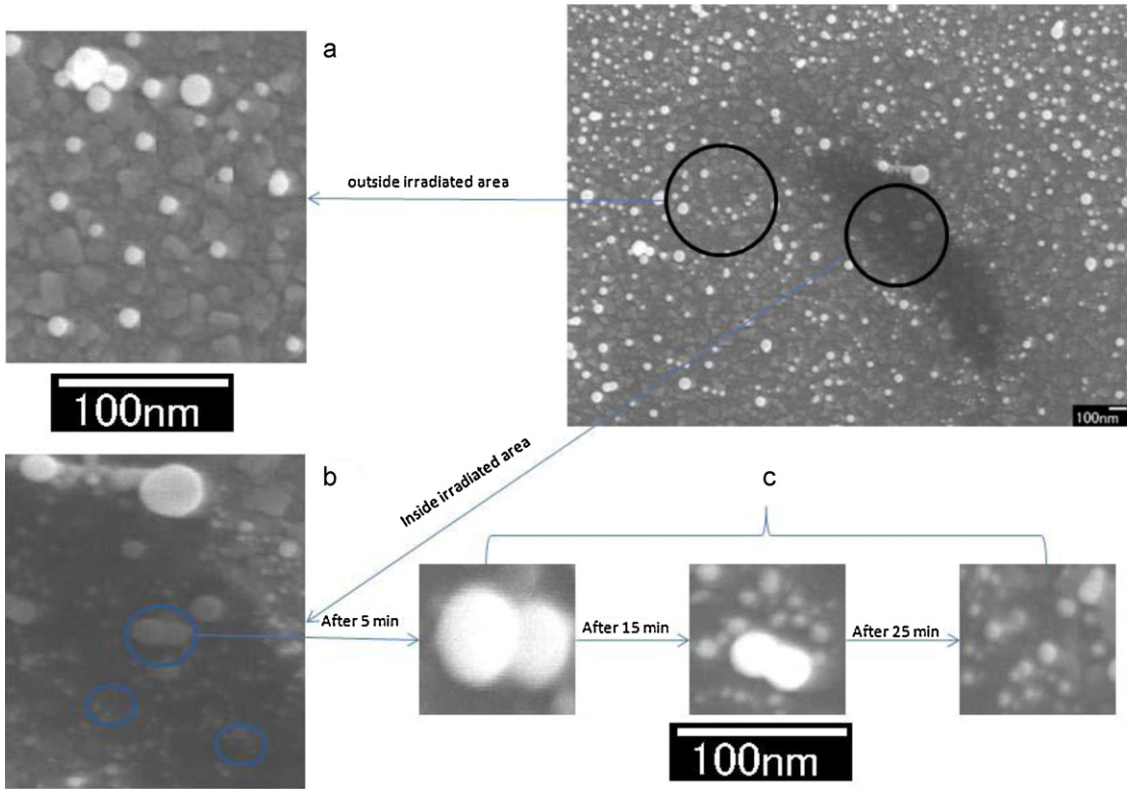

Fig. 5. FE-SEM images of silver nanoparticles on ITO surface (50 Ω/sq). FE-SEM images of Ag-NPs (a) outside and (b) inside the irradiated area. (c) The kinetic development of a narrow spherical Ag-NPs on ITO surface at different irradiation time (5, 15 and 25 min).

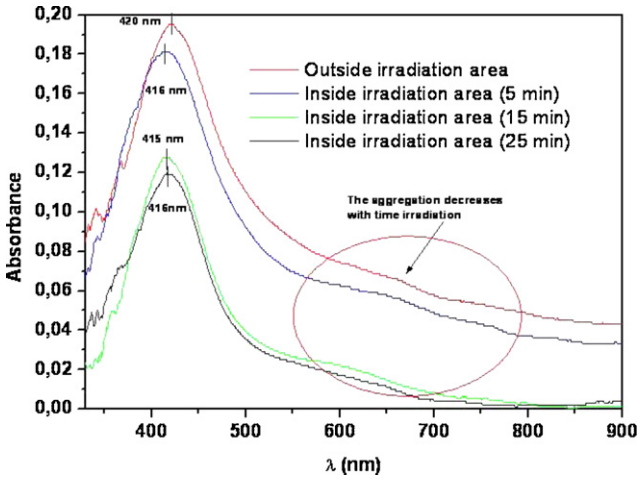

Fig. 6. UV/vis absorbance spectroscopy of Ag/ITO (50 Ω/sq) outside and inside the irradiated area. The absorbance curve shows that the aggregation and the SPR maximum decreases with irradiation time.

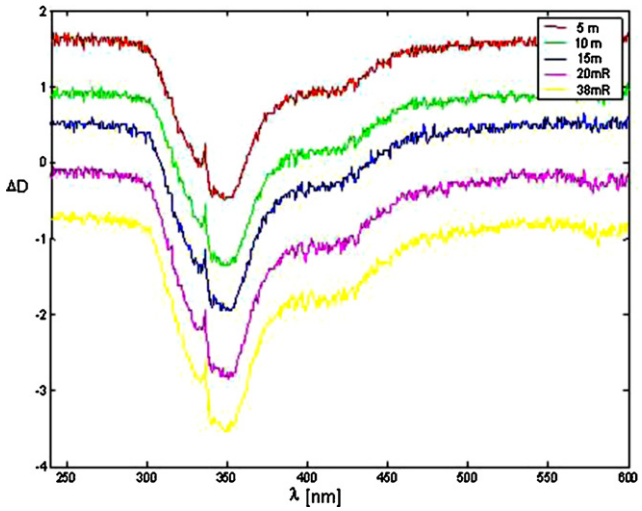

Fig. 7. Photoinudced changes of absorption for the 50 Ω/sq Ag NP/ITO after different times of treatment. The curves indicated 20 mR and 38 mR correspond to the photo-induced absorption after interruption of the Nd: YAG 532 nm-laser treatment.

increase in particle size. Such a process is somewhat hindered by the substrate roughness. As the film roughness increases, the contact angle increases and the initial seeds find themselves entrapped in narrow and separated regions. During the growth step, the resulting particles undergo Van Der Waals and Oswald ripening only at the available valleys of the surface. External photoinduced filed which is near the surface plasmon resonance maxima may lead to substantial re-distribution of the inter-particle interaction both due to the photothermal processes as well as due to effective interactions with the plasmons. As a consequence, depending on the time of the treatment we observed different steps of the photoinduced process. In Refs. [2,8] also it was shown that the photoinduced creation of the crystal-shaped particles occurs even by longer wavelength (700 nm) irradiation which indicates the photo-irradiation might control the interaction between silver atoms and the nanoparticles surface *via* electronic field excitation rather than the reduction rate of silver ions. Several roles in the process of the photoinduced changes of the morphology may also account photoinduced nonlinear optical processes due to enhanced local field inside and near Ag nanoparticles under the surface plasmon resonance condition [9].

Further, maximum changes are observed at wavelength about 349 nm, which is close to the maximum 330 nm of photoluminescence for bulk silver [10], however it is noteworthy that the Ag NP show the photoluminescence at about 330 nm [11]. Thus one can

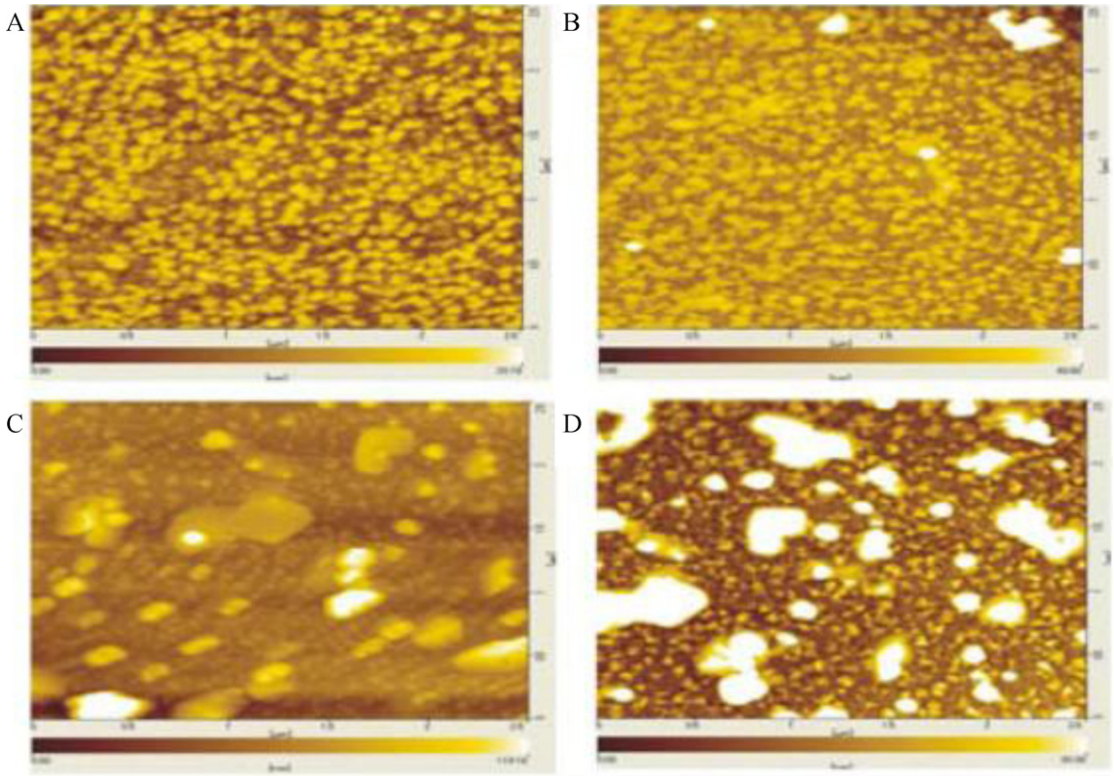

Fig. 8. AFM images of (A) non-irradiated ITO-50 Ω/sq; (B) ITO-50 Ω after irradiation 5 min; (C) ITO-50 Ω after irradiation 15 min and (D) ITO-50 Ω after irradiation 25 min.

expect that the observed changes are superimposed on the inter-band d→sp Ag transitions and here we observed the effects caused mainly by the photopolarization due to inter-band interactions, which remain even after the interrupting of the laser excitations. The spectral changes in absorption which are observed at about 430 nm are relatively mainly caused by surface plasmon resonance maxima of the NP [12,13]. Following the obtained data, with an illumination by 532 nm wavelength we excited the trapping levels which are readily available for the effective interaction with the surface plasmon resonance peaks. As a consequence even after the interruption of the interactions between the external electromagnetic field and local electric field we have observed the enhanced process which continues to exist. We have coupled charged trapping states which are effectively interacting with the inter-band and SPR states [14]. The obtained results are in agreement with the data observed in Ref. [15] also with two principal bands.

4. Conclusions

In this study, the photo-induced absorption using the pulsed 30 ps, 532 nm doubled frequency Nd:YAG laser, we have established that there occur some drastic changes in the absorption within the spectral range 340–360 nm. The changes are higher for the relatively higher resistance sheet. We found that the maximum changes are observed at wavelength about 349 nm, which is close to the maximum 330 nm of photoluminescence for bulk silver; however it is interesting that the Ag NP show the photoluminescence at about 330 nm. Thus one can expect that the observed changes are superimposed on the inter-band d→sp Ag transitions and here we observed the effect caused mainly by the photopolarization determined by inter-band interactions, which remain even after the interrupting of the excitations. The spectral changes in the absorption which are observed at about 430 nm are relatively mainly caused by surface plasmon resonance maxima for the NP. Even after the interruption of the interactions between the external electromagnetic field and local electric field we have noticed the enhanced process which continues to exist. This could be as a consequence of coupled charged trapping states which are effectively interacting with the inter-band and SPR states. The morphological changes monitored by AFM show drastically increases of the Ag NP aggregations, which are responsible for the kinetics of the photo-induced treatments for such types of samples.

References

[1] L.L. Yang, X.D. He, F. He, Y.B. Li, S. Zhang, T. An, W.T. Zheng, Thin Solid Films 517 (2009) 4979.
[2] K. Nouneh, M. Oyama, R. Diaz, M. Abd-Lefdil, I.V. Kityk, M. Bousmina, J. Alloys Compd. 509 (2011) 2631.
[3] C. Guillén, J. Herrero, Opt. Commun. 282 (2009) 574.
[4] I.V. Kityk, J. Ebothé, K. Ozga, K.J. Plucinski, G. Chang, Kobayashi, M. Oyama, Physica E 31 (2006) 38.
[5] J. Ebothé, R. Miedziński, A.H. Reshak, K. Nouneh, M. Oyama, A. Aloufy, M. El Messiry, Mater. Chem. Phys. 113 (2009) 187.
[6] R. Miedziński, J. Ebothé, G. Kozlowski, J. Kasperczyk, I.V. Kityk, I. Fuks-Janczarek, K. Nouneh, M. Oyama, M. Matusiewicz, A.H. Reshak, Superlatt. Microstruct. 46 (2009) 637.
[7] G. Chang, J. Zhang, M. Oyama, K. Hirao, J. Phys. Chem. B 109 (2005) 1204.
[8] T. Tsuji, Y. Okazaki, M. Tsuji, J. Photochem. Photobiol. Chem. A 194 (2008) 247.
[9] D. Yan, S.J. Chin, Phys. Lett. 27 (2010) 024204.
[10] P. Apell, R. Monreal, S. Lundquist, Phys. Scr. 38 (1988) 174.
[11] A.P. Zhang, J.Z. Zhang, Y. Fang, J. Lumin. 128 (2008) 1635.
[12] D. Basak, S. Karan, B. Mallik, Chem. Phys. Lett. 420 (2006) 115.
[13] A.V. Akimov, A. Mukherjee, C.L. Yu, D.E. Chang, A.S. Zibrov, P.R. Hemmer, H. Park, M.D. Lukin, Nature 450 (2007) 402.
[14] G.T. Boyd, Z.H. Yu, Y.R. Shen, Phys. Rev. B 33 (1986) 7923.
[15] O.A. Yeshchenko, I.M. Dmitruk, A.A. Alexeenko, M.Y. Losytskyy, A.V. Kotko, A.O. Pinchuk, Phys. Rev. B 79 (2009) 235438.